

Supplementary Information

Safe and high-rate supercapacitors based on “acetonitrile/water in salt” hybrid electrolyte

Qingyun Dou,^{ac} Shulai Lei,^a Da-Wei Wang,^b Qingnuan Zhang,^a Dewei Xiao,^{ad}
Hongwei Guo,^{ae} Aiping Wang,^{fg} Hui Yang,^h Yongle Li,^h Siqi Shi^{fg} and Xingbin Yan^{*a}

^a Laboratory of Clean Energy Chemistry and Materials, State Key Laboratory of Solid Lubrication,
Lanzhou Institute of Chemical Physics, Chinese Academy of Sciences, Lanzhou 730000, P. R.
China

^b School of Chemical Engineering, The University of New South Wales, Sydney, NSW 2052,
Australia

^c University of Chinese Academy of Sciences, Beijing 100039, P. R. China

^d School of Materials Science and Engineering, Anhui University of Technology, Ma'anshan,
243000, P.R. China

^e Department of Chemical Engineering and Technology, School of Petrochemical Engineering,
Lanzhou University of Technology, Lanzhou 730050, P.R. China

^f School of Materials Science and Engineering, Shanghai University, Shanghai 200444, P.R. China.

^g Materials Genome Institute, Shanghai University, Shanghai 200444, P.R. China.

^h Department of physics, International center for quantum and molecular structures, and Shanghai
Key Laboratory of High Temperature Superconductors, Shanghai 200444, P.R. China.

E-mail: xbyan@licp.cas.cn

Experimental Sections

Materials and Characterization

Preparation of “acetonitrile/water in salt” (AWIS) electrolytes: In a typical synthesis, lithium bis (trifluoromethane sulfonyl) imide (LiTFSI, 0.0420 mol, 12.06 g) was mixed with distilled water (H₂O, 0.111 mol, 2.00 g) at 25 °C to create a 21 m solution, which was then diluted by stoichiometric amount of acetonitrile (CH₃CN; 0.0244 mol, 1.0 g; 0.0537 mol, 2.2 g; 0.0976 mol, 4.0 g; 0.156 mol, 6.4 g; 0.293 mol, 12.0 g) to formulate AWIS electrolytes with concentrations of 14, 10, 7, 5 and 3 m. Conductivity was measured by a conductivity meter (DDS-307, YuePing, Shanghai). Viscosity was measured by a kinematic viscosity testing device (SYP1003-III). Diffusivities of lithium (D_{Li}) and fluorine (D_{F}) were measured by pulsed-field-gradient nuclear magnetic resonance (pfg-NMR) on a Bruker Avance 600 MHz spectrometer. Flammability tests were performed by igniting the electrolytes (~ 0.1 g) soaked in glass fibers. The self-extinguishing time (SET) was calculated by normalizing the time from the flame to self-extinguish by the electrolyte mass. Raman spectra were measured using a Lab Ram HR Evolution series High Resolution Raman Spectrometer (HORIBA Jobin Yvon SAS, France). Commercial activated carbon (AC, YP-50F, Kuraray Chemical, Japan) was annealed under argon atmosphere at 700 °C for 3 h prior to use. Scanning electron microscope (SEM) was performed using a microscope (JEOL JSM 6701 F). Nitrogen adsorption-desorption isotherm was performed on a porosimeter (Micromeritics, ASAP 2020M) at 77 K. The surface chemical species of cycled anode were examined on X-ray photoelectron spectroscopy (XPS, ESCALAB250x) using 1486.6 eV Al K α radiation as the excitation source. The anode was recovered from a SC after three cycles at an operation voltage of 2.2 V, and then washed with acetonitrile and dried under vacuum.

Electrode Preparation and Electrochemical Measurements

Preparation of AC electrodes: 95 wt% AC powder (1.5 mg) was homogeneously mixed with 5 wt% poly(tetrafluoroethylene) (PTFE, aqueous solution) and drops of ethanol to create a paste, which was pressed onto the stainless steel wire current collector at 10 MPa. The AC electrodes were dried at 60 °C for 2 h under vacuum. Three-electrode system: An AC electrode (with a mass loading of 1.5 mg) as the working electrode, another AC electrode (with a high mass loading of 7.5 mg) as the counter electrode, Ag/AgCl electrode as the reference electrode. Symmetric supercapacitors (SCs) were assembled in coin cell with two identical YP-50F electrodes with a glass fiber as the separator. Linear sweep voltammetry, cyclic voltammetry (CV), galvanostatic charge/discharge (GCD) and electrochemical impedance spectroscopy (EIS) tests were performed using an electrochemical workstation (CHI660E, Shanghai, China). Linear sweep voltammetry was scanned from the open circuit potential to positive and negative polarization limits (± 1.8 V versus Ag/AgCl). Each CV and GCD test was firstly cycled ten times to make sure a steady state of the system before recording data. EIS was recorded from 0.01 to 100 kHz. Cycling performance was tested using a LAND system (CTA2001A, Wuhan Land Electronic Co. Ltd.). The characterization of the respective potential ranges of positive and negative electrodes in a SC was achieved by introducing an Ag/AgCl (in 1.0 M KCl solution) reference electrode using two electrochemical workstations (Princeton, VersaSTAT, USA). A temperature/humidity chamber (Dongguan Kowin Testing Equipment Co. Ltd.) was used to provide the constant temperature environment for electrochemical tests.

The specific capacitance C (F g^{-1}) of CV curves was calculated by equation (1):

$$C = \frac{\int_0^{V/s} j dt}{V} \quad (1)$$

where j is the gravimetric current density (A g^{-1}), s is the scan rate (V s^{-1}), and V is the operation voltage (V).

The specific capacitance C (F g^{-1}) of the device was calculated from GCD curves by equation (2):

$$C = \frac{j \cdot \Delta t}{V} \quad (2)$$

where Δt (s) is the discharge time.

Reduction potential predicted from quantum chemistry calculation

The $\text{Li}^+(\text{CH}_3\text{CN})$ and LiTFSI aggregates and free TFSI^- were chosen as study objects because they are representative clusters in 5 m AWIS electrolyte as found in DFT-MD simulations (Figure 2d). The predicted reduction potential of free TFSI^- has been reported (1.4 V versus Li/Li^+).¹ In this study, we calculated the reduction potential of the other two complexes, $\text{Li}^+(\text{CH}_3\text{CN})$ and LiTFSI , using the G4MP2 and B3LYP/6-31+G(d) methodology, respectively. All the calculations were implemented in Gaussian 09 suite.^{1,2} The SMD solvation model with the parameter input of water was used in the calculation. Here we use A to denote the complex of interest. The reduction potential of the complex A was calculated as the negative of the free energy of A^- formed in solution ($\Delta G_{298}^{\text{S}} = G_{298}^{\text{S}}(\text{A}^-) - G_{298}^{\text{S}}(\text{A})$) divided by the Faraday constant ($E = -\Delta G_{298}^{\text{S}} / e - 1.4$ versus Li/Li^+).

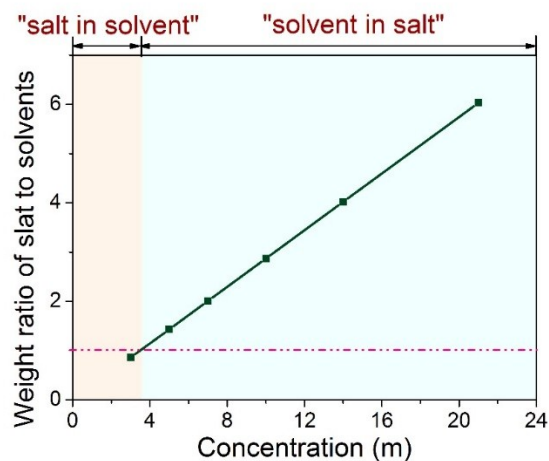


Figure S1. The weight ratio of salt (LiTFSI) to solvents (acetonitrile/water) as a function of the concentrations for various AWIS electrolytes.

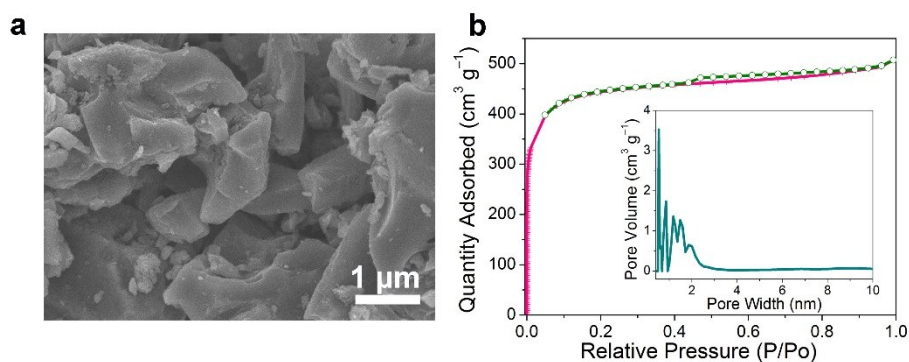


Figure S2. Characterization of YP-50F activated carbon. a) A typical scanning electron microscope (SEM) image. b) Nitrogen adsorption-desorption isotherm.

Table S1. Diffusivities of lithium (D_{Li}) and fluorine (D_F) measured by 7Li NMR and ^{19}F NMR in the 5 m AWIS and 21 m WIS electrolytes.^{2,3}

	D_{Li} ($m^2 s^{-1}$)	D_F ($m^2 s^{-1}$)
5 m AWIS	3.02×10^{-10}	2.24×10^{-10}
21 m WIS	5.15×10^{-11}	1.98×10^{-11}

The lithium transference number (t_{Li}) of 5 m AWIS electrolyte was 0.58, which was derived from the diffusivities:

$$t_{Li} = \frac{D_{Li}}{D_{Li} + D_F} \quad (3)$$

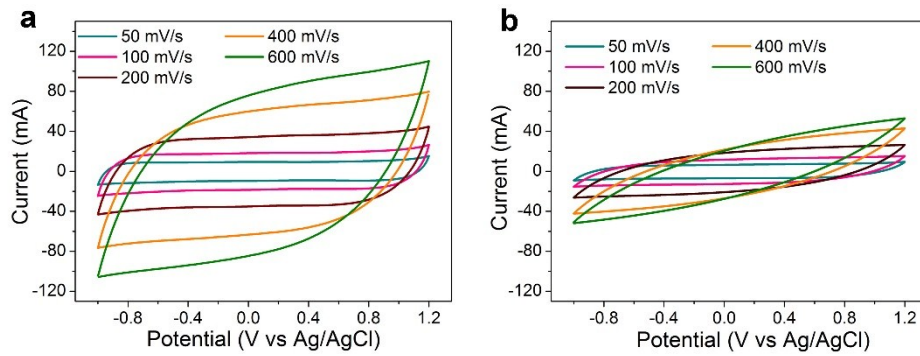


Figure S3. CV curves of YP-50F electrode in a) 5 m AWIS electrolyte and b) 21 m WIS electrolyte at an operating potential window of -1.0 to 1.2 V versus Ag/AgCl at different scan rates.

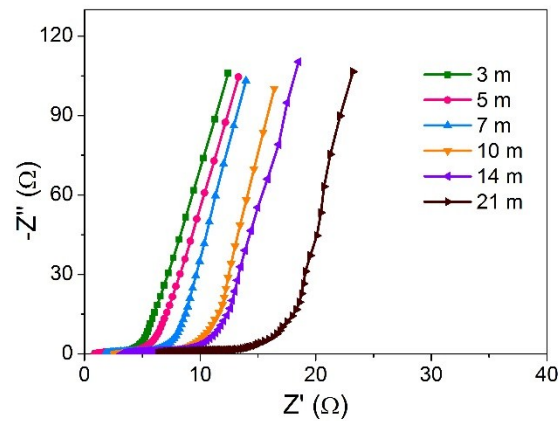


Figure S4. Nyquist plots of YP-50F electrode in various electrolytes.

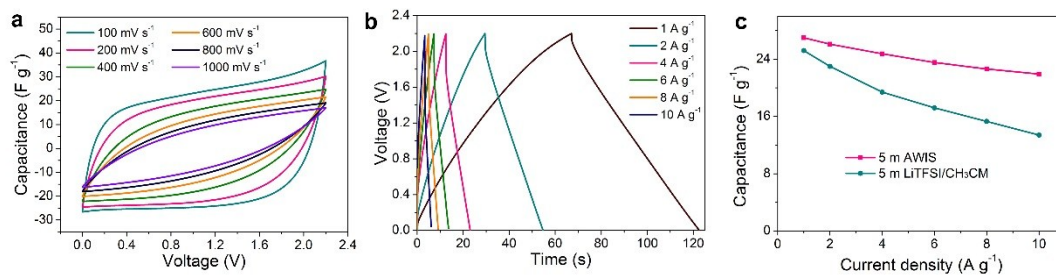


Figure S5. a) CV curves at different scan rates and b) GCD curves at different current densities of the SC using 5 m LiTFSI/CH₃CN electrolyte. c) Comparison of the specific capacitance of the SCs using 5 m AWIS electrolyte and the SC using 5 m LiTFSI/CH₃CN electrolyte at different current densities.

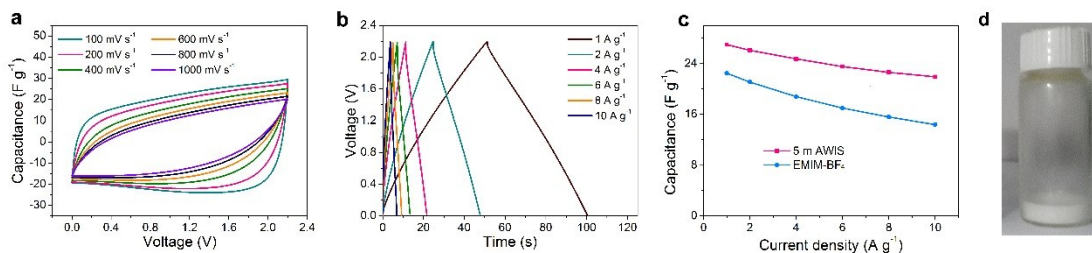


Figure S6. a) CV curves of the SC using EMIM-BF₄ at different scan rates. b) GCD curves of the SC using EMIM-BF₄ at different current densities. c) Comparison of the specific capacitance of the SCs using 5 m AWIS electrolyte and the SC using EMIM-BF₄ at different current densities. d) Photographs showing the state of EMIM-BF₄ at -25 °C.

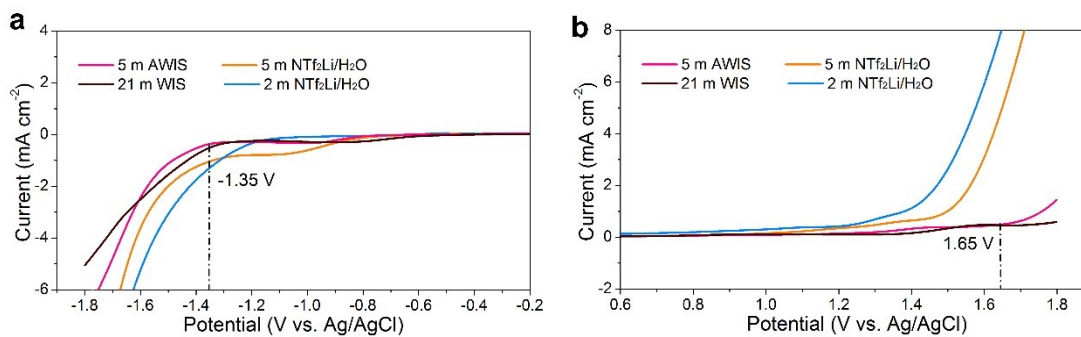


Figure S7. Magnifications near a) cathodic and b) anodic limits of the electrochemical stability windows for various electrolytes determined by linear sweep voltammetry tests at a scan rate of 20 mV s⁻¹. In this system, a value of 0.5 mA cm⁻² was defined as the threshold for electrolyte decomposition.

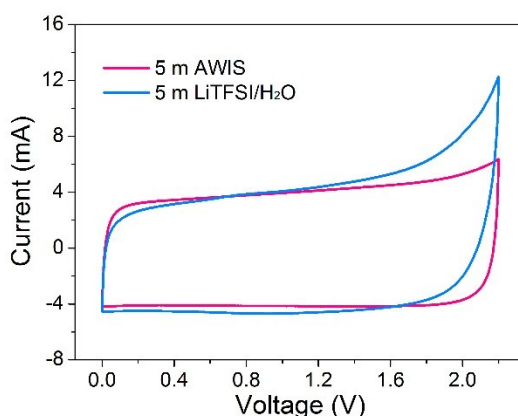


Figure S8. Comparison of the CV curves of the SC using 5 m AWIS electrolyte and the SC using 5 m LiTFSI/H₂O electrolyte at an operation voltage of 2.2 V at a scan rate of 50 mV s⁻¹.

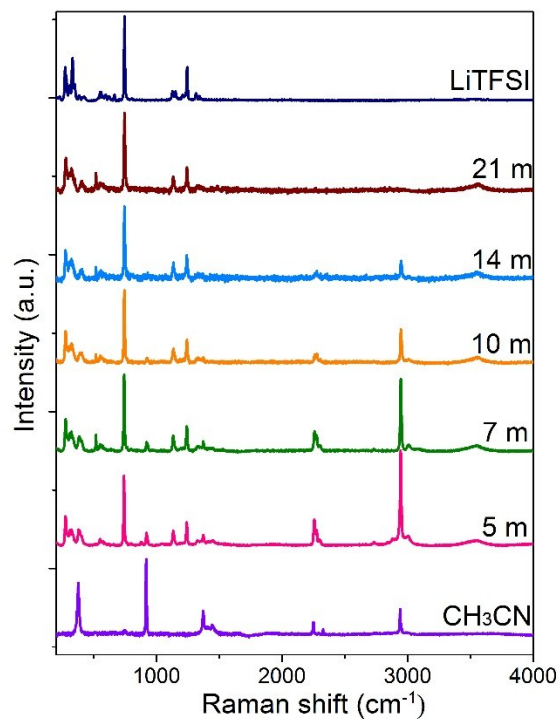


Figure S9. Raman spectra of 21 m WIS electrolyte and various AWIS electrolytes with crystalline LiTFSI and liquid acetonitrile as the reference.

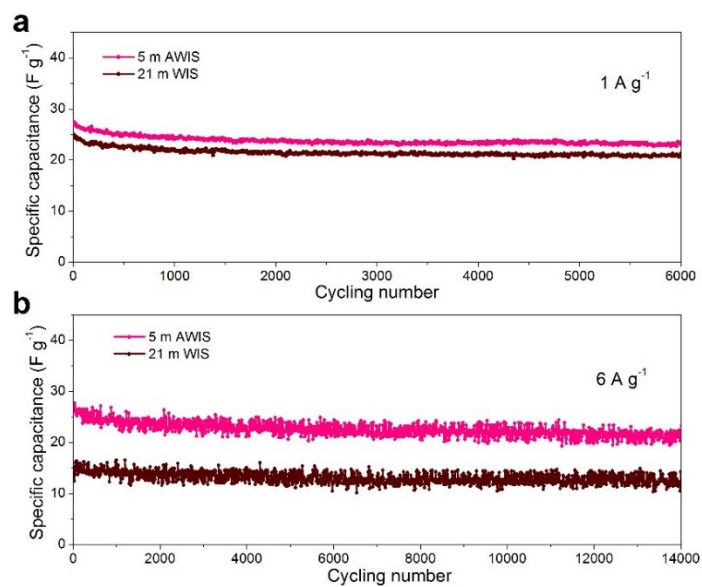


Figure S10. Comparison of cycling performance of the SC using 5 m AWIS electrolyte and the SC using 21 m WIS electrolyte at an operation voltage of 2.2 V at current densities of a) 1 A g⁻¹ and b) 6 A g⁻¹.

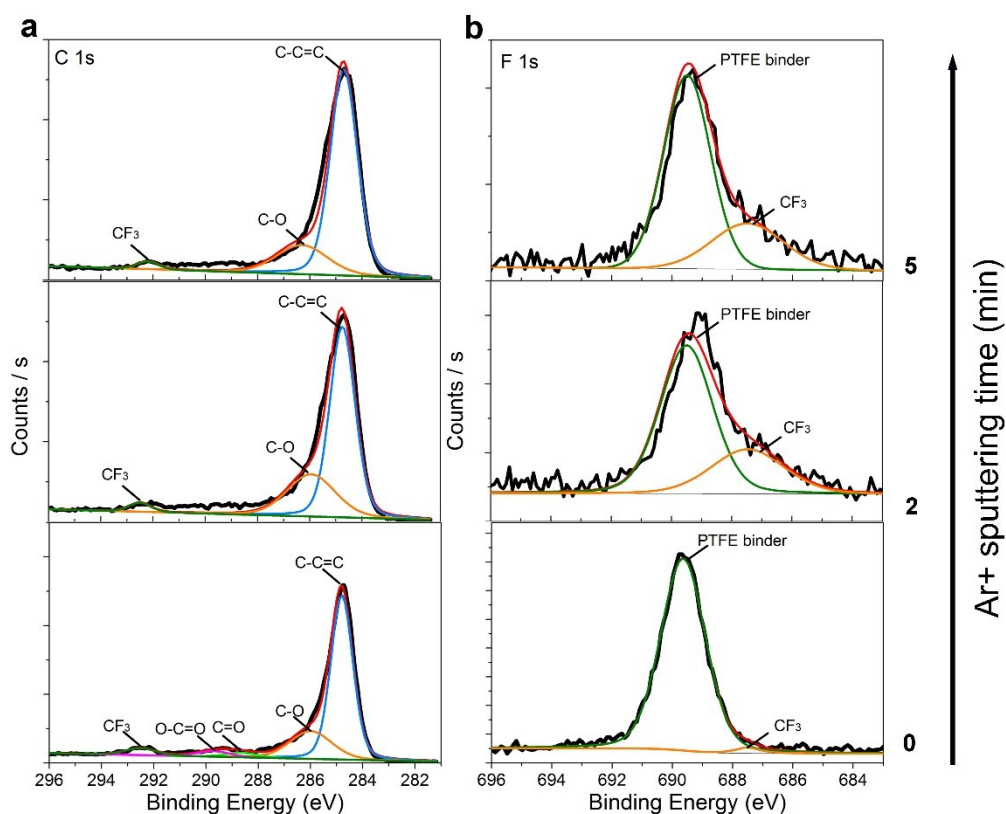


Figure S11. XPS spectra of SC anode in 5 m AWIS electrolyte after three charging/discharging cycles. a) The evolution of C 1s and b) the evolution of F 1s during Ar⁺ sputtering.

The C 1s peak can be deconvoluted into five peaks, among these, 284.8 (C=C-C), 286.7 (C-O), 288.3 (C=O) and 289.7 eV (O-C=O) are typical signals for carbons,⁴ while 292.3 eV (CF₃) should come from a small amount of remaining TFSI anions.¹ The F 1s peak can be deconvoluted into two peaks: 689.5 eV come from PTFE binder and 687.5 eV (CF₃) come from the remaining TFSI anions.¹ Note that there was not the peak for LiF (685.7 eV). After etching the top layer of the sample by Ar⁺, the signal for LiF was still not found. Thus, these results indicate that LiF-based SEI was not formed in the anode electrode in our system.

Table S2. Predicted reduction potentials of Li⁺(CH₃CN) and LiTFSI aggregates.

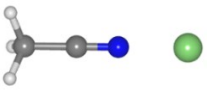
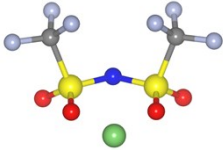
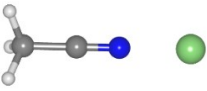
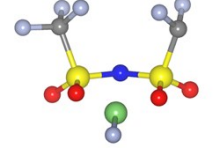
Aggregates	Li ⁺ (CH ₃ CN)	LiTFSI
Before reduction		
After reduction		
Reduction potential	$\Delta G_{298}^S = G_{298}^S(A^-) - G_{298}^S(A)$ $= -35.283 \text{ kcal mol}^{-1}$ $E = -\Delta G_{298}^S / e - 1.4 = 0.13$ <p>V versus Li/Li⁺</p>	$\Delta G_{298}^S = G_{298}^S(A^-) - G_{298}^S(A)$ $= -84.24 \text{ kcal mol}^{-1}$ $E = -\Delta G_{298}^S / e - 1.4 = 2.25$ <p>V versus Li/Li⁺</p>



Figure S12. Photographs showing the state of 21 m WIS electrolyte at different temperatures.



Figure S13. Photographs showing the state of 5 m AWIS electrolyte at -50 °C.

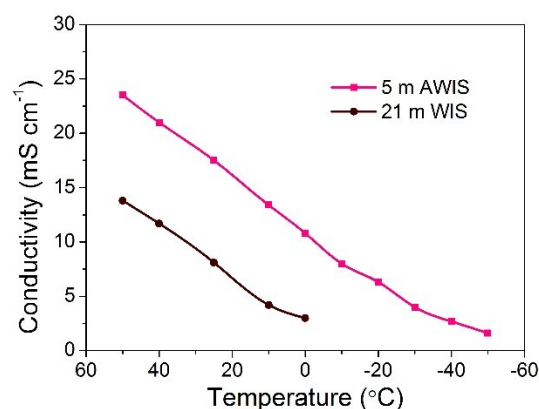


Figure S14. Conductivities of 5 m AWIS electrolyte and 21 m WIS electrolyte at different temperatures. Note that salts precipitated in the 21m WIS electrolyte below 10 °C during conductivity measurement.

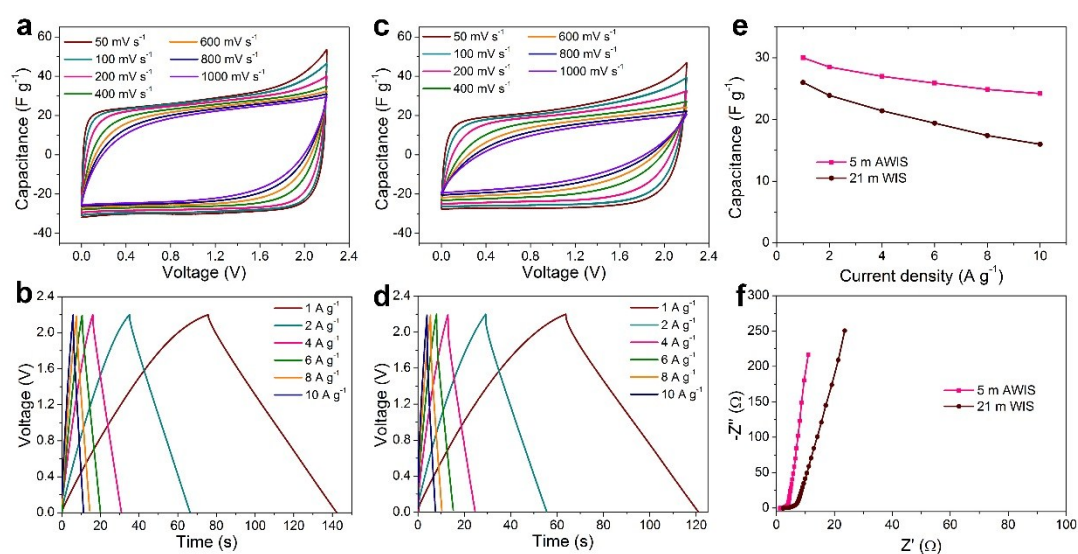


Figure S15. a) CV curves at different scan rates and b) GCD curves at different current densities of the SC using 5 m AWIS electrolyte at 50 °C. c) CV curves at different scan rates and d) GCD curves at different current densities of the SC using 21 m WIS electrolyte at 50 °C. e) Comparison of the specific capacitance at different current densities at 50 °C. f) Nyquist plots of the SCs using different electrolytes at 50 °C.

References

- 1 L. Suo, O. Borodin, T. Gao, M. Olguin, J. Ho, X. Fan, C. Luo, C. Wang and K. Xu, *Science*, 2015, **350**, 938.
- 2 F. Wang, O. Borodin, M. S. Ding, M. Gobet, J. Vatamanu, X. Fan, T. Gao, N. Edison, Y. Liang, W. Sun, S. Greenbaum, K. Xu and C. Wang, *Joule*, 2018, **2**, 927.
- 3 O. Borodin, L. Suo, M. Gobet, X. Ren, F. Wang, A. Faraone, J. Peng, M. Olguin, M. Schroeder, M. S. Ding, E. Gobrogge, A. von Wald Cresce, S. Munoz, J. A. Dura, S. Greenbaum, C. Wang and K. Xu, *ACS Nano*, 2017, **11**, 10462.
- 4 J. Chen, G. Zhang, B. Luo, D. Sun, X. Yan and Q. Xue, *Carbon*, 2011, **49**, 3141.